Mitotic checkpoint proteins HsMAD1 and HsMAD2 are associated with nuclear pore complexes in interphase

Michael S. Campbell, Gordon K. T. Chan and Tim J. Yen*

Fox Chase Cancer Center, 7701 Burholme Ave., Philadelphia, PA 19111, USA

*Author for correspondence (e-mail: tj_yen@fccc.edu)

Accepted 19 December 2000

Journal of Cell Science 114, 953-963 © The Company of Biologists Ltd

SUMMARY

Mad1 was first identified in budding yeast as an essential component of the checkpoint system that monitors spindle assembly in mitosis and prevents premature anaphase onset. Using antibodies to the human homologue of Mad1 (HsMAD1), we have begun to characterize this protein in mammalian cells. HsMad1 is found localized at kinetochores in mitosis. The labeling is brightest in prometaphase and is absent from kinetochores at metaphase and anaphase. In cells where most chromosomes have reached the metaphase plate, those aligned at the plate show no labeling while remaining, unaligned chromosomes are still brightly labeled. We find HsMad1 associated with HsMad2. Association with p55CDC, a protein previously shown to bind HsMad2, was not detected. Surprisingly, unlike any other known mitotic checkpoint proteins, HsMad1 and HsMAD2 were found localized at nuclear pores throughout interphase. This was confirmed by co-labeling with an antibody to known nuclear pore complex proteins and by their co-purification with enriched nuclear envelope fractions. HsMad1 was identified serendipitously by its binding to a viral protein, HTLV-1 Tax, which affects transcription of viral and human proteins. The localization of HsMad1 to nuclear pore complexes suggests an alternate, non-mitotic role for the Mad1/Tax interaction in the viral transformation of cells.

Key words: Nuclear pore complex, MAD1, MAD2, Kinetochore, Checkpoint

INTRODUCTION

The mitotic checkpoint is a regulatory mechanism that prevents aneuploidy by delaying sister chromatid separation before all chromosomes have aligned at the metaphase plate. Following nuclear envelope breakdown, chromosomes must attach to microtubules of the forming mitotic spindle through structures called kinetochores. Each chromosome has two kinetochores on opposite sides of the centromere, one on each sister chromatid. Once both kinetochores attach to spindle microtubules, chromosomes migrate towards the equator of the spindle through a series of saltatory movements to form the metaphase plate. Due to the stochastic nature by which chromosomes become attached to the spindle, some chromosomes become aligned before others. To ensure that cells at this stage of mitosis do not prematurely enter anaphase with unaligned chromosomes, the checkpoint detects the presence of unaligned chromosomes and delays anaphase onset. Only after all chromosomes have properly aligned is the signal given to separate sister chromatids and drive cells into anaphase. Thus, the checkpoint prevents premature anaphase that would otherwise lead to aneuploidy.

It has become increasingly clear that kinetochores are at the crossroads of the complex signaling pathways that comprise the mitotic checkpoint. Laser ablation studies have demonstrated that unattached kinetochores are the source of an inhibitor of anaphase onset (Rieder et al., 1995). In a process that is not completely understood, the tension exerted on the kinetochore by bilateral microtubule attachments downregulates the inhibitory signal (Li and Nicklas, 1995). Once all chromosomes have aligned and their kinetochores are under maximal tension, the inhibitor decays and anaphase can begin.

The molecular components of the mitotic checkpoint pathway were discovered in yeast by identification of mutants that failed to arrest in mitosis in the presence of microtubule drugs. Six genes named Mad1, 2 and 3 (Li and Murray, 1991) and BUB1, 2, 3 (Hoyt et al., 1991) were identified by this approach. A seventh gene, encoding Mps1 kinase, was initially identified as essential for spindle pole body functions (Winey et al., 1991) but was also found to be essential for the mitotic checkpoint (Weiss and Winey, 1996). Discovery of the yeast checkpoint genes led to the identification of their metazoan orthologs. Combined studies from yeast and higher organisms have led to an emerging picture of checkpoint function. Mad1, 2, 3 and Bub1 and Bub3 exhibit extensive interactions, localize to kinetochores in metazoans, and are members of a common pathway that senses kinetochore-microtubule attachments and prevents premature separation of sister chromatids (reviewed by Taylor, 1999). Bub2, in contrast, is located at spindle pole bodies and is thought to exert its checkpoint function after chromatid separation through a different pathway (Fraschini et al., 1991; Fesquet et al., 1999; Alexandru et al., 1999).

Mad1p was found to be a nuclear phosphoprotein in yeast (Hardwick and Murray, 1995), and its function in the mitotic checkpoint is dependent on its association with the Mad2 protein. Interestingly, this association persists throughout the cell cycle (Chen et al., 1999). The *Xenopus* homologues

Xmad1 (Chen et al., 1998) and Xmad2 (Chen et al., 1996) have been shown to be essential for the mitotic checkpoint in egg extracts. Both Xmad1 and Xmad2 accumulate at unattached kinetochores where they are thought to participate in generating the inhibitory signal to block anaphase. Immunodepletion and add back studies led Chen et al. to propose that Xmad1 specifies the association between Mad2 and kinetochores (Chen et al., 1998). At the kinetochore, Xmad2 is postulated to be converted, through an unknown mechanism, to a form that can inhibit anaphase onset. This model is partly supported by genetic and biochemical data that show recombinant MAD2 can bind to and inhibit the anaphase promoting complex/cyclosome (APC/C), a multi-subunit protein complex that ubiquitinates proteins that must be destroyed to allow sister chromatid separation (reviewed by Fang et al., 1999; Hershko, 1999).

TXBP181 cDNA was isolated from a yeast two-hybrid screen for proteins that interact with the Tax protein from the human retrovirus HTLV-I (Jin et al., 1998). Examination of its sequence revealed TXBP181 to be a human ortholog of MAD1. In support of this, transfected TXBP181 fusion proteins were able to bind HsMAD2. Furthermore, transfection of a mutant TXBP181 lacking the ability to bind HsMAD2 disrupted mitotic checkpoint function and led to a profusion of multinucleated cells. However, the results from studies conducted with an antibody raised against the carboxy-terminal 18 residues predicted from TXBP181 cDNA were inconsistent with the properties ascribed to Xmad1. Western blots with this antibody identified a ~150 kDa protein that was much larger than expected from the cDNA sequence while antibodies against Xmad1 cross-reacted with a human protein of ~85 kDa (Chen et al., 1998). In addition to this, the peptide antibody to TXBP181 failed to stain kinetochores as would be expected for a checkpoint protein.

To resolve the discrepancy between TXBP181 and Xmad1, we independently cloned a human MAD1 cDNA from HeLa cells and generated antibodies against bacterial fusion proteins expressing separate domains of HsMAD1. Our antibodies recognize a single protein of ~85 kDa that is close to the size calculated from our cDNA sequence and to the size of the human protein recognized by anti-Xmad1 antibodies (Chen et al., 1998). Further confirmation that our antibodies recognized HsMAD1 was obtained when they co-immunoprecipitated HsMAD2 from cell lysates. Genetic and biochemical studies have shown that MAD2 can associate with Cdc20, a protein that specifies substrate recognition by the APC/C but is also thought to target MAD2 to the APC/C. We find that HsMAD2 forms a complex with HsMAD1 but we were unable to detect p55CDC, the mammalian homologue of Cdc20, in association with this complex. Consistent with Xmad1 and other mitotic checkpoint proteins, HsMAD1 preferentially localized to unattached kinetochores during mitosis. Perhaps our most intriguing finding was that both HsMAD1 and HsMAD2 localize to the nuclear pore complex throughout interphase. We present evidence locating HsMAD1 on the nucleoplasmic face of the pore and discuss the implications of kinetochore checkpoint proteins at nuclear pores. We also propose the possibility that, in addition to interfering with mitotic checkpoint function, the transforming Tax protein may affect nuclear pore function and transport by binding to HsMAD1.

MATERIALS AND METHODS

Cell culture, transfections and drug treatment

HeLa cells were grown in DMEM supplemented with 5% FBS, 20 mM Hepes, 60 μg/ml penicillin, and 100 μg/ml streptomycin. Cells were grown in a humidified 37°C chamber with 5% CO_2. Cells were blocked in mitosis with 0.02 μg/ml nocodazole (Sigma, St Louis, MO) for 18 hours. Cells blocked in S phase were obtained by incubating 18 hours in 2 mM thymidine (Sigma), rinsing out the drug, and replacing it after 12 hours for an additional 18 hours. Mitotic cells were harvested (after nocodazole block) or eliminated (after thymidine block) by irrigation with a pipet. Cells growing on coverslips or in dishes were transfected using FuGENE 6 as directed by the manufacturer (Boehringer Mannheim).

Cloning and antibodies

5′-CATGGAAGACCTGGGGGAAAACACCATGGT and 3′-TTT-CACAAGGTGAGGAACCCAGGCTGGTGG terminal primers derived from the published sequence of TXBP181 (Jin et al., 1998) (GenBank accession number U33822) were used to amplify MAD1 from a HeLa Marathon cDNA library (Clontech). This was ligated into the Topo-TA vector (Invitrogen), which was used for DNA sequencing and as a template to prepare full length MAD1 with restriction sites at the ends. Upon sequencing, we noted a discrepancy between the cDNA we cloned and the sequence of TXBP181 (U33822). Our cDNA contained a single additional nucleotide (C) between positions 2162 and 2163 of TXBP181. This insertion had the effect of changing the reading frame after this point and resulted in a predicted open reading frame of 718 amino acids as opposed to 803 amino acids for TXBP181. Thus a new primer (5′-TGCAA-GCTTCGCCACGGTCTGGCGGCTGAA-3′) was used to amplify the complete coding sequence of HsMAD1 (2154 base pairs coding for 718 amino acids). This construct was ligated into a GST fusion vector for expression in mammalian cells. A fragment representing amino acids 331-718 of the HsMAD1 protein was cloned into a pGEX bacterial expression vector for protein production. Following induction with 2 mM IPTG, bacteria were lysed in 50 mM Na_2PO_4, 5 mM $MgCl_2$, 200 mM NaCl, 0.1 mg/ml lysozyme. Lysate was frozen on dry ice, thawed at 55°C, sonicated 5 minutes, and centrifuged at 70,000 ***g***. A portion of the pellet was dissolved in gel sample buffer and run on a 10% acrylamide gel. After Coomassie staining, the band containing the expressed HsMAD1 fragment was excised and used to immunize a rat and a rabbit.

The same fragment of HsMAD1 was also cloned into a pMAL MBP fusion vector (New England Biolabs, Beverly, MA) that was also used for protein production as above. After sonication and centrifugation, a Coomassie stained gel revealed that the MBP-MAD1 fusion was the predominant protein in the insoluble pellet. The pellet was solubilized in 125 mM Tris-HCl, pH 6.8, 2% SDS and dialyzed overnight at 4°C against 100 mM Hepes, pH 8.0, 250 mM NaCl. The dialyzed sample was then coupled to Affi-Gel 10 immunoaffinity support (Bio-Rad, Richmond, CA) as described in the manufacturer's directions. Serum from immunized animals was first passed twice over a GST column. The flow through from this column was then passed over the MBP-MAD1 immunoaffinity column. Antibodies were eluted with 0.5% acetic acid, 150 mM NaCl and immediately neutralized with 1 M Tris-HCl, pH 8.5. Purified antibodies were concentrated in a Centricon 30 (Amicon, Beverly, MA) and stored in 50% glycerol, 25 mM Tris-HCl, pH 7.5, at –20°C.

Immunoprecipitation and western blotting

Cells were rinsed in PBS and lysed in NP-40 lysis buffer (1% NP-40, 50 mM Tris-HCl, pH 7.5, 150 mM NaCl, 1 mM DTT). Cell lysates were centrifuged at 10,000 ***g*** at 4°C for 5 minutes. The protein concentrations of the lysates were determined (BCA protein assay; Pierce Chemical Co.). Immunoprecipitation was performed with 300 μg of lysate. Rat anti-HsMAD1, mouse anti-HsMAD2 (Transduction

Laboratories), or rabbit anti-p55CDC was added to a final concentration of ~2 μg/ml. Lysates were incubated with antibodies for 2 hours at 4°C, and then 75 μl of 50% slurry of Protein A– or Protein G-Sepharose (Repligen, Cambridge, MA) was added and the incubation continued for another 30 minutes. GST-MAD1 fusion protein was purified from cell lysates using glutathione Sepharose beads (Pharmacia). The beads were recovered by low speed centrifugation and washed four times in 0.5 ml of ice-cold NP-40 lysis buffer before SDS gel sample buffer was added. Samples from the immunoprecipitates or whole cell lysates were separated through 8% or 8-15% gradient SDS-PAGE and transferred onto Immobilon P (Millipore).

Membranes were blocked overnight at 4°C in 5% bovine serum albumin in 50 mM Tris-HCl, pH 8.0, 150 mM NaCl, 0.05% Tween-20 (TBST). Primary antibodies were diluted in the same buffer and incubated with membranes for two hours at room temperature. After rinsing, membranes were incubated 30 minutes with the appropriate secondary antibodies conjugated to alkaline phosphatase (Sigma). Membranes were rinsed in TBST then in 100 mM diethanolamine, pH 10, 1 mM $MgCl_2$. CSPD substrate solution (Tropix) was added and the membranes exposed to film.

Immunofluorescence labeling and imaging

Cells on coverslips were rinsed briefly in 60 mM PIPES, 25 mM HEPES, pH 6.9, 10 mM EGTA, and 4 mM $MgCl_2$ (PHEM) and extracted 4 minutes in 1% CHAPS detergent in PHEM. Cells were then fixed 12 minutes in 1% paraformaldehyde in PHEM and rinsed three times in 10 mM MOPS, pH 7.4, 150 mM NaCl, 0.05% Tween-20 (MBST). For differential permeabilization, cells were treated with 0.004% digitonin in MBS for 15 minutes at 4°C. Purified HsMAD1 and mAb414 ascites (Davis and Blobel, 1986) (Covance, Richmond, CA) were diluted 1/4000, rabbit anti-HsMAD2 serum (provided by E. D. Salmon) was diluted 1/30, and anti-GST (Santa Cruz Biotechnology) and rabbit anti-Nup93 (provided by J. VanDeursen) were diluted 1/1000 in MBST with 5% calf serum. Primary incubations were for 1 hour at 37°C. Cy3 and Cy2 or FITC conjugated secondary antibodies (Jackson Immunoresearch) were diluted 1/400 in the same buffer. Secondary incubations were for 30 minutes at 37°C. For differential permeabilization experiments, antibodies were diluted in PBS with 5% calf serum. Cells were rinsed briefly in 0.2 μM Yo-Pro1 (Molecular Probes, Eugene, OR) or 0.1 μg/ml DAPI (Sigma) to visualize DNA before mounting in Vectashield (Vector Labs, Burlingame, CA). Images were taken on a Nikon Microphot SA with a ×100 PlanNeofluor objective and TEC-1 CCD camera (Dage-MTI) controlled with IP LabSpectrum v2.0.1 (Scanalytics Inc.).

Electron microscopy

HeLa cells growing on coverslips were rinsed with PHEM and then equal amounts of 1% CHAPS detergent and 1% glutaraldehyde in PHEM were added simultaneously. After 4 minutes this solution was aspirated and replaced with 0.5% glutaraldehyde in PHEM for 10 more minutes. Cells were rinsed and immunolabeled with anti-HsMAD1 antibody at 1/100 for 2 hours at room temperature. Secondary incubation was performed for 2 hours using Nanogold 1.4 nm gold-conjugated Protein G (Nanoprobes, Stony Brook, NY) at a 1/30 dilution. Samples were postfixed 1 hour in 2% glutaraldehyde, rinsed thoroughly in water, and gold particles were enlarged using the Nanoprobes HQ-silver enhancement kit. Coverslips were rinsed, stained 15 minutes in 0.1% OsO_4 in water, dehydrated through ethanol and propylene oxide, and embedded in EPON.

Nuclear envelope preparation

HL60 cells were suspended in 250 mM sucrose, 50 mM Tris-HCl, pH 7.4, 5 mM $MgSO_4$ and mechanically lysed with a Dounce homogenizer. Nuclei and nuclear envelopes were then isolated as described (Kaufmann et al., 1983). Rat liver nuclear envelopes were prepared as described (Mahajan et al., 1998).

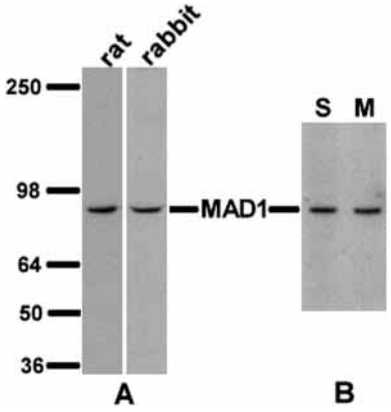

Fig. 1. Anti-HsMAD1 expression does not vary between S phase and mitosis. (A) Western blots of HeLa lysates prepared from asynchronous cells were probed with affinity purified rat and rabbit polyclonal anti-HsMAD1 antibodies. Both antibodies specifically recognize a 83 kDa protein of the predicted size of HsMAD1. (B) Levels of HsMAD1 protein remain relatively unchanged between thymidine-blocked interphase cells (lane 1) and nocodazole-blocked mitotic cells (lane 2). Equal cell numbers were loaded in each lane.

RESULTS

HsMAD1 antibodies recognize a 83 kDa human protein

Although the human MAD1 checkpoint protein has been described previously (Jin et al., 1998), we sought to characterize it in greater detail. Based on the published sequence of human TXBP181, we made primers and cloned HsMAD1 from a HeLa cDNA library by PCR. Comparison of our HsMAD1 cDNA sequence to the published sequence of TXBP181 (GenBank U33822) showed that our cDNA had a single nucleotide insertion between nucleotide positions 2162 and 2163 of the TXBP181 cDNA. Subsequent MAD1 sequences deposited by the same group (AF083811; AF083812) and others (AF123318) also contain the identical insertion, suggesting the original TXBP181 sequence was incorrect. This single nucleotide insertion alters the reading frame of the TXBP181 sequence to produce a shorter open reading frame that encodes a predicted polypeptide of 718 amino acids and 83 kDa rather than 803 amino acids and 97 kDa that was predicted from the TXBP181 cDNA. The sequence we cloned is equivalent to GenBank AF123318. The change in predicted amino acid sequence encoded by our HsMAD1 cDNA resulted in an increased percentage homology, relative to the TXBP181 cDNA, to *Saccharomyces cerevisiae*, *Schizosaccharomyces pombe* and *Xenopus laevis* MAD1 (not shown).

To characterize the endogenous HsMAD1, we made and affinity purified rat and rabbit polyclonal antibodies against a fragment corresponding to amino acids 331-718 of the human MAD1 protein. Our antibodies recognize a single band of ~83 kDa that is close to the calculated size of HsMAD1 (Fig. 1A). We did not see a band that migrated in the 150 kDa range that was previously reported to be TXBP181 (Jin et al., 1998). Although Jin et al. failed to address the discrepancy between the 150 kDa band on western blots and the predicted size of TXBP181 of 97 kDa (Jin et al., 1998), we believe it is due to

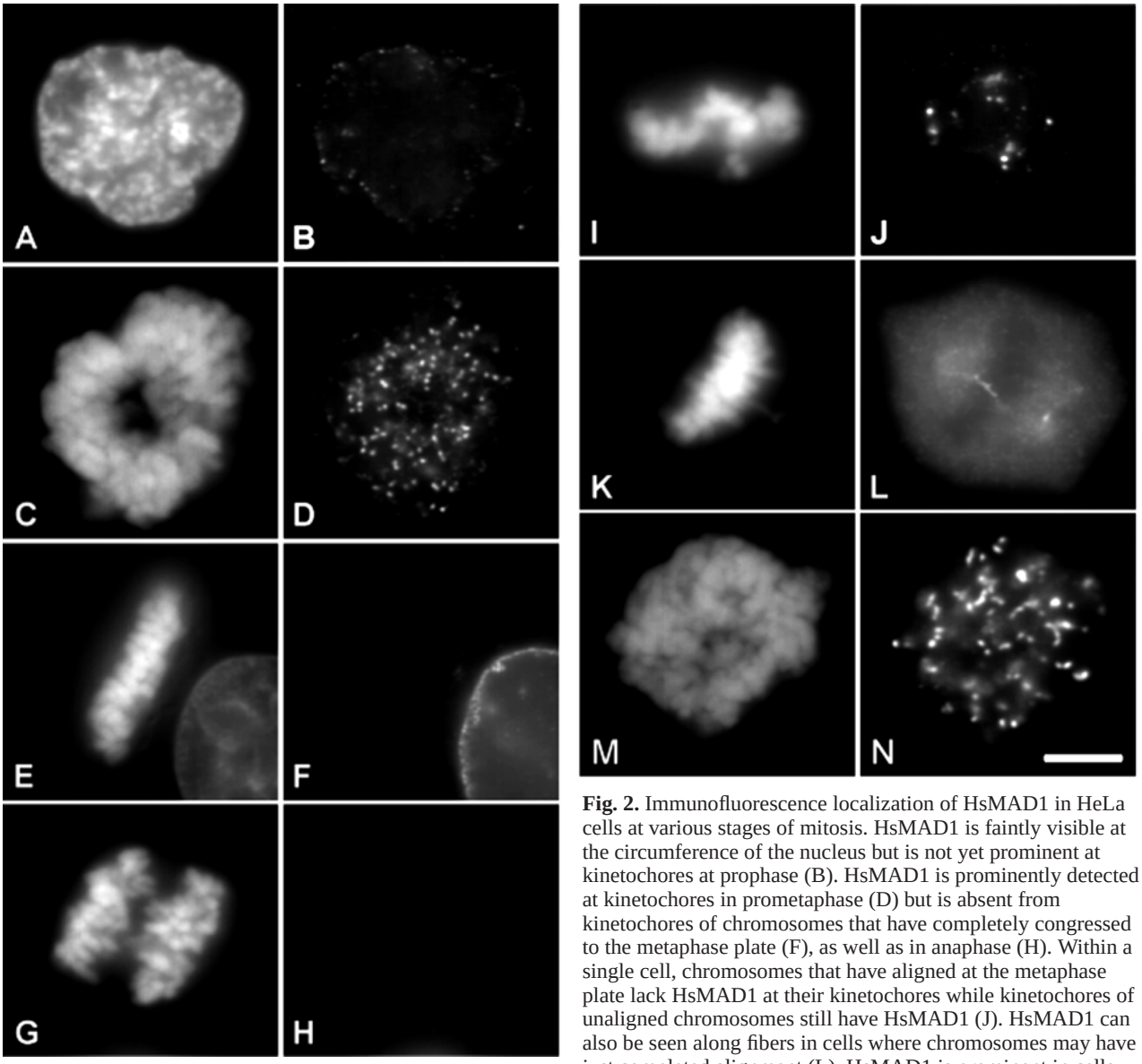

Fig. 2. Immunofluorescence localization of HsMAD1 in HeLa cells at various stages of mitosis. HsMAD1 is faintly visible at the circumference of the nucleus but is not yet prominent at kinetochores at prophase (B). HsMAD1 is prominently detected at kinetochores in prometaphase (D) but is absent from kinetochores of chromosomes that have completely congressed to the metaphase plate (F), as well as in anaphase (H). Within a single cell, chromosomes that have aligned at the metaphase plate lack HsMAD1 at their kinetochores while kinetochores of unaligned chromosomes still have HsMAD1 (J). HsMAD1 can also be seen along fibers in cells where chromosomes may have just completed alignment (L). HsMAD1 is prominent in cells treated with nocodazole (N). Cells were pre-extracted, fixed and then stained with rat anti-hsMAD1 antibodies followed with Cy3 anti-rat secondary. Chromosomes were visualized with YoPro (A,C,E,G,I,K,M). Bar, 5 μm.

the antibody used. It was raised against the predicted C-terminal 18 amino acids of TXBP181. However, due to the sequencing error, this peptide does not exist within the actual HsMAD1 protein. Thus, the 150 kDa band on western blots is likely to be some other protein unrelated to HsMAD1.

Since the levels of some mitotic checkpoint proteins vary throughout the cell cycle, typically peaking in mitosis, we sought to determine whether this was the case for HsMAD1. The amount of HsMAD1 was compared in S-phase and mitotic cells and found to be the same (Fig. 1B). Thus it appears that HsMAD1 protein levels do not fluctuate between S and M.

Immunofluorescence staining was used to determine the intracellular localization of HsMAD1. We labeled HeLa cells with anti-HsMAD1 antibodies and examined cells in different stages of mitosis. Similar results were obtained with both rat and rabbit antibodies and cells labeled with the rat antibodies are shown. In prophase, before nuclear envelope breakdown, HsMAD1 appears in punctate dots at the nuclear periphery (Fig. 2A and B). Kinetochore localization of HsMAD1 becomes apparent in prometaphase, which follows nuclear envelope breakdown (Fig. 2C and D). HsMAD1 remains at kinetochores until they align at the spindle equator in metaphase. From metaphase through telophase, HsMAD1 is no longer detectable at kinetochores (Fig. 2E-H). As is the case with other checkpoint proteins, differences in HsMAD1 levels can be detected among kinetochores within the same cell. In late prometaphase, chromosomes that have not completely congressed to the metaphase plate still have HsMAD1 at their kinetochores, while those aligned at the plate have lost it (Fig. 2I and J). HsMAD1 can be seen, usually in discrete packets, along spindle microtubules (Fig. 2K and L). Treatment of cells with the microtubule inhibitor

nocodazole results in bright labeling of all kinetochores (Fig. 2M and N).

HsMAD1 interacts with HsMAD2

It has been shown that the checkpoint protein HsMAD2, in conjunction with p55CDC, can bind to the APC/C and inhibit its ubiquitinating activity (Wassmann and Benezra, 1998; Kallio et al., 1998). It is also clear that Mad2 can bind to Mad1 in both yeast (Chen et al., 1999) and *Xenopus* (Chen et al., 1998). Consistent with this data, HsMAD1 immunoprecipitates also contain HsMAD2 protein (Fig. 3A, lane 1). The reciprocal experiment was also performed, confirming that HsMAD2 immunoprecipitates contain HsMAD1 (lane 2). Although HsMAD2 was present in p55CDC immunoprecipitates, HsMAD1 was not detected (lane 3) and remained in the supernatant (lane 4). A non-immune IgG precipitate does not contain HsMAD1 or HsMAD2 (lane 5).

To further confirm the interaction between HsMAD1 and HsMAD2, a GST-HsMAD1 fusion construct was made and transfected into HeLa cells. Native HsMAD1 from an untransfected cell lysate is seen in Fig. 3B, lane 1. A lysate prepared from transfected cells was immunoprecipitated with HsMAD1 antibodies and blotted for HsMAD1 (lane 2). Both the native HsMAD1 and the GST-HsMAD1 fusion protein can be seen. In addition, lysate from transfected cells was precipitated with glutathione-Sepharose beads and the beads were found to selectively recover the GST-HsMAD1 fusion protein but not endogenous HsMAD1 (lane 3). Nevertheless, the GST-HsMAD1 fusion protein was able to associate with endogenous HsMAD2 (Fig. 3C).

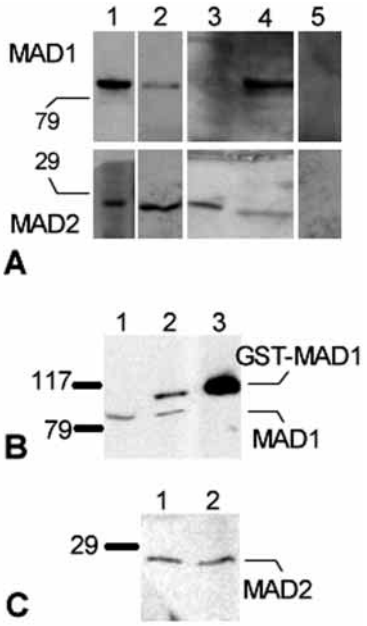

Fig. 3. Characterization of HsMAD1 protein interactions in HeLa cells. (A) HsMAD1 interacts with HsMAD2 but not p55CDC. HsMAD1 (lane 1), HsMAD2 (lane 2), and p55CDC (lane 3) immunoprecipitates were western blotted with anti-HsMAD1 (top) and anti-HsMAD2 (bottom) antibodies. p55CDC-depleted supernatant (lane 4) and control immunoprecipitate (lane 5) are also shown. (B) MAD1 does not form homo-oligomers. A western blot of untransfected extract (lane 1), anti-MAD1 immunoprecipitate (lane 2) or glutathione Sepharose precipitate (lane 3) prepared from cells transfected with GST-MAD1 was probed with anti-HsMAD1 antibodies. (C) MAD2 associates with GST-MAD1. Western blot with anti-HsMAD2 antibodies against lysate prepared from untransfected cells (lane 1) and glutathione beads incubated in lysate prepared from cells transfected with GST-MAD1 (lane 2).

HsMAD1 is at nuclear pores in interphase

Examination of the interphase staining pattern obtained with our HsMAD1 antibodies showed a ring of HsMAD1 labeling around the entire circumference of the nucleus (Fig. 4A). While we cannot rule out the possibility that there is some HsMAD1 in the interior of the nucleus, we believe the majority of the signal within the nucleus is due to out of focus peripheral labeling from above and below the plane of focus. There was no evidence of HsMAD1 labeling of interphase centromeres as was previously suggested (Jin et al., 1998). Focusing on the top or bottom surfaces of the nucleus reveals a speckled pattern of HsMAD1 labeling (Fig. 4B). Hundreds of tiny dots cover the entire surface of the nucleus. This was reminiscent of the size and distribution of nuclear pore complexes (NPCs). To confirm this we co-labeled cells with monoclonal antibody 414 (mAb414), which recognizes several known NPC proteins (Davis and Blobel, 1986). The patterns of staining obtained with mAb414 and HsMAD1 were nearly identical as demonstrated when the two images are merged (Fig. 4B, merged). An enlargement of the nuclear pore labeling is shown in Fig. 4C. This demonstrates that HsMAD1 co-localizes with nuclear pore complexes. All interphase cells exhibit this pattern of labeling, so the presence of HsMAD1 at NPCs is not cell cycle dependent.

To rule out the possibility that the NPC labeling was due to non-specificity of our antibody, the localization of a transfected GST-HsMAD1 was determined. Six hours after transfection cells were detergent extracted, fixed, and labeled with anti-GST antibodies to localize the expressed fusion protein. As shown in Fig. 4D, the GST-HsMAD1 produces a punctate staining very similar to that obtained with HsMAD1 or mAb414 antibodies.

To obtain biochemical support for the association between HsMAD1 and NPCs, we probed for its presence in nuclear envelope preparations prepared from rat livers and human HL60 cells. Our antibodies recognize HsMAD1 present in the isolated nuclei (Fig. 4E, lanes 1). The nuclei were then treated with nucleases and extracted with salt. This extracted fraction contains little or no detectable HsMAD1 (Fig. 4E, lanes 2). The bulk of the HsMAD1 is recovered in the remaining fraction, which is highly enriched in nuclear envelopes (Fig. 4E, lanes 3). This demonstrates that HsMAD1 is a tightly associated component of the nuclear envelope.

Certain detergents will permeabilize the cell membrane, but not the nuclear envelope (Pante et al., 1994). To determine whether HsMAD1 is located on the nucleoplasmic or cytoplasmic face of the NPC, cells were extracted with either CHAPS or digitonin. HsMAD1 pore labeling is routinely seen when cells are extracted with 1% CHAPS, which permeabilizes the nuclear envelope (Fig. 5A and B). Digitonin, on the other hand, permeabilizes the cell membrane but not the nuclear envelope. When cells are extracted only with digitonin, no HsMAD1 NPC labeling is observed (Fig. 5C and D). In this situation, the anti-HsMAD1 antibodies can enter the cytoplasm

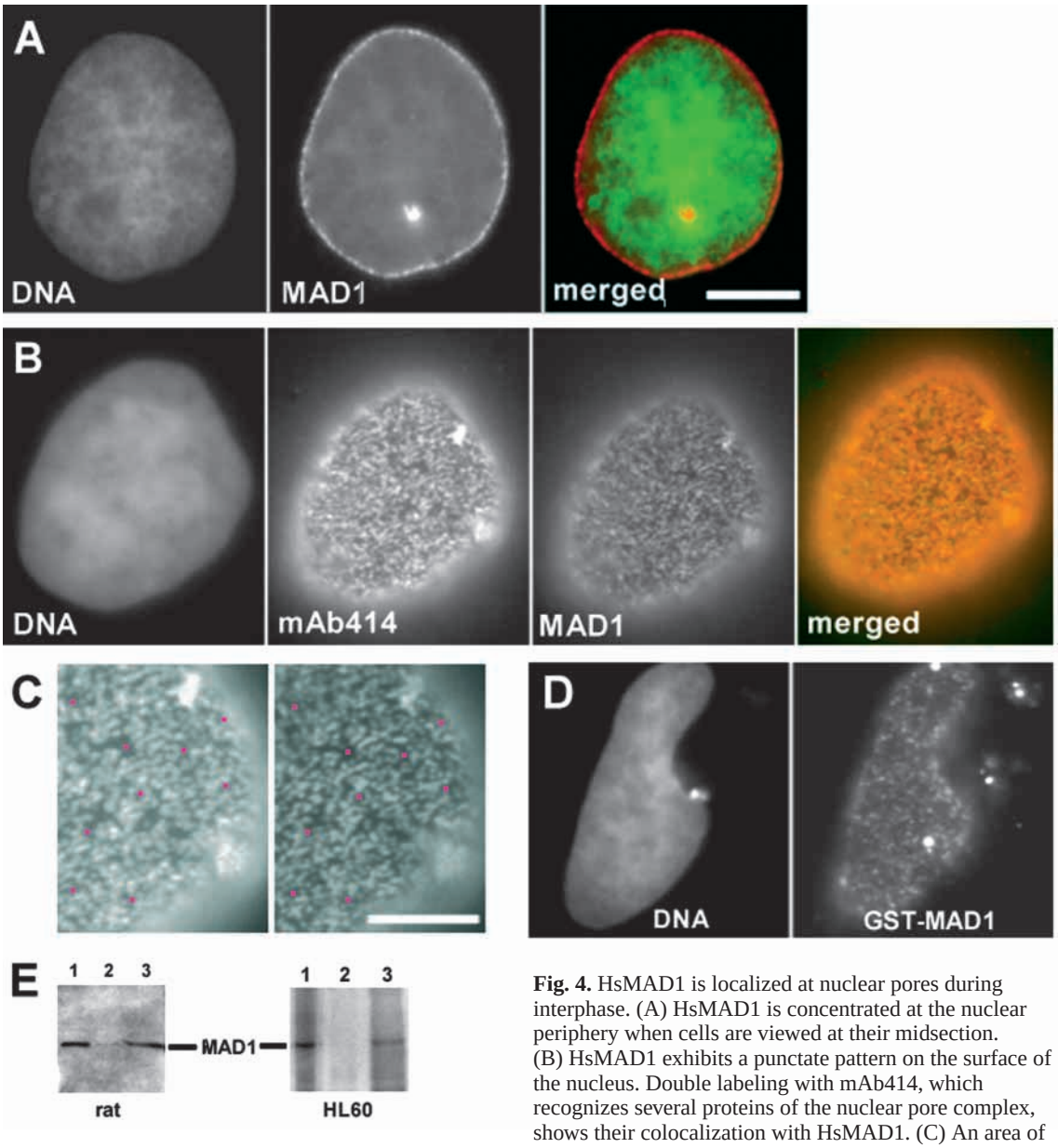

Fig. 4. HsMAD1 is localized at nuclear pores during interphase. (A) HsMAD1 is concentrated at the nuclear periphery when cells are viewed at their midsection. (B) HsMAD1 exhibits a punctate pattern on the surface of the nucleus. Double labeling with mAb414, which recognizes several proteins of the nuclear pore complex, shows their colocalization with HsMAD1. (C) An area of the cell shown in (B) was enlarged to show mAb414 (left) and HsMAD1 (right) labeling in more detail, with purple dots shown to aid in registration. (D) HeLa cells were transfected with a GST-HsMAD1 fusion construct and processed for immunofluorescence 6 hours later. Anti-GST antibody labeling reveals localization of the fusion protein to nuclear pores. Bar, 5 μm (A,B,D are the same scale). (E) Biochemical fractionation of nuclei prepared from rat liver (lanes 1 to 3) or HL60 (lanes 4 to 6) cells shows that HsMAD1 co-fractionates with nuclear envelope components. Western blots of whole nuclei (lanes 1, 4), nuclease treated, salt extracted supernatant (lanes 2, 5), and highly enriched nuclear envelope fractions (lanes 3, 6) were probed for HsMAD1. Each lane was loaded with equal cell equivalents of samples for comparison.

but cannot penetrate inside the nucleus. As a control, digitonin permeabilized cells were also labeled with mAb414, which recognizes proteins present on the cytoplasmic face of the nuclear envelope. Bright pore labeling was obtained in this case (Fig. 5E and F). The absence of labeling in digitonin permeabilized cells suggests that HsMAD1 is likely to be located on the nucleoplasmic side of the NPC.

To get a more detailed picture of the location of HsMAD1 within the NPC, we performed immunoelectron microscopy. The NPC comprises a cylindrical structure with octagonal symmetry in the plane of the nuclear envelope. The central channel defined by the octagonal structure contains the central transporter. In addition, filaments extend from the complex above and below the plane of the nuclear envelope. On the nucleoplasmic side, these filaments converge in a conical shape to form a basket-like structure beneath the pore (reviewed by Bodoor et al., 1999). In views where the nuclear envelope was perpendicular to the plane of section (Fig. 6, insets A and B), HsMAD1 is indeed found at NPCs and is clearly located inside the nucleus and not on the cytoplasmic side, in confirmation of

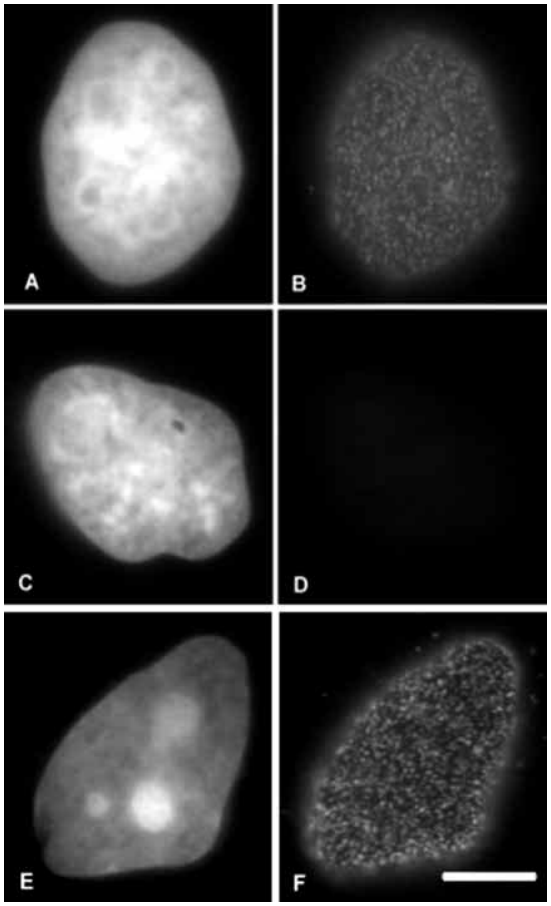

Fig. 5. HsMAD1 is on the nuclear side of the nuclear envelope. HsMAD1 staining of cells extracted with the detergent CHAPS (A and B), which permeabilizes the nuclear envelope, produces pore labeling. No MAD1 staining is detected when cells are extracted with digitonin (C and D), which permeabilizes the cell membrane but not the nuclear envelope. MAb414, which labels proteins on the cytoplasmic face of the nuclear envelope, still labels cells permeabilized with digitonin (E and F). DNA was stained with DAPI (A,C,E). HsMAD1 was detected with rat anti-HsMAD1 and Cy3 anti-rat secondary (B and D). MAb414 was secondary labeled with Cy3 anti-mouse antibody (F). Bar, 5 μm.

the digitonin results described above. In most cases, the gold particles representing HsMAD1 extend from the pore into the nucleus. HsMAD1 label is never detected within the plane of the nuclear envelope. It is sometimes possible to obtain a view in which the nuclear envelope is parallel to the plane of section and the NPCs can be seen en face (Fig. 6). In these cases, HsMAD1 label is not at the circumference of the octameric pore structure itself, but appears to coincide with the channel.

HsMAD2 colocalizes with HsMAD1 at nuclear pore complexes

Our work, as well as that of others, has shown that HsMAD1 associates with HsMAD2. In budding yeast, this association continues throughout the cell cycle (Chen et al., 1999). We have shown here that HsMAD1 is found at nuclear pores throughout interphase. Further, Chen et al. reported that Mad1 and Mad2 are present at *Xenopus* nuclear envelopes. Thus, we wanted to determine whether the HsMAD2 at nuclear envelopes was actually coincident with HsMAD1 at NPCs. HeLa cells were fixed and double labeled with rat anti-HsMAD1 and rabbit anti-HsMAD2 antibodies. As shown in Fig. 7A, HsMAD2 gives a very similar staining pattern to HsMAD1, hundreds of dots on the surface of the nuclear envelope. As with HsMAD1, this pattern of HsMAD2 localization is detected throughout interphase. Overlaying HsMAD1 and HsMAD2 labeling results in good colocalization of the two proteins. HsMAD2 co-localizes with HsMAD1 at the nuclear pore complex. To biochemically confirm HsMAD2's association with the nuclear envelope, enriched nuclear envelope preparations from HL60 cells were probed for this protein. As with HsMAD1, HsMAD2 remains associated with nuclease and salt extracted nuclear envelopes (Fig. 7C, lane 3).

HsMAD1 overexpression induces annulate lamellae formation

We showed that when a GST-HsMAD1 construct is expressed in HeLa cells the fusion protein localizes to NPCs after six hours (Fig. 4). When examined 24-36 hours after transfection, cells show a different pattern of fusion protein localization. Staining with anti-GST antibodies reveals the GST-HsMAD1 protein localized to vesicular structures present throughout the cell. These structures are not observed in untransfected cells. They range in shape from small to large spheres to more extensive tubular structures. They were reminiscent of annulate lamellae, an incompletely characterized organelle found in many types of cells consisting of membrane cisternae containing numerous structures that are morphologically and biochemically very similar to nuclear pore complexes (reviewed by Kessel, 1992). Further, overexpression of a NPC protein has previously been shown to induce formation of annulate lamellae (Imreh and Hallberg, 2000). To determine whether the HsMAD1-containing structures observed in GST-HsMAD1 transfected cells were akin to annulate lamellae, we stained with antibodies to other NPC proteins. Nup93 has been shown to localize to the nuclear basket component of the NPC, where our electron microscopy data suggest HsMAD1 is located. As shown in Fig. 8B, Nup93 localizes to the structures in a punctate pattern suggesting it is labeling pore-like structures. We also detected labeling of the structures with mAb414, although the pattern is different (Fig. 8D). The NPC proteins recognized by this antibody are present as single patches on spherical vesicles and, interestingly, in between vesicles that appear to be fusing together (Fig. 8D, arrows). We showed that HsMAD2 is present at NPCs, and labeling of transfected cells revealed that it is also present in a punctate pattern on the fusion protein-induced structures (Fig. 8F). Since they contain several other NPC proteins, we conclude the structures are equivalent to annulate lamellae. Thus, overexpression of the single NPC protein HsMAD1 is sufficient to induce formation of annulate lamellae containing other known NPC proteins.

DISCUSSION

Results obtained with our HsMAD1 antibodies are consistent with those obtained for Xmad1 but contrast significantly with those obtained with TXBP181 antibodies. The discrepancies

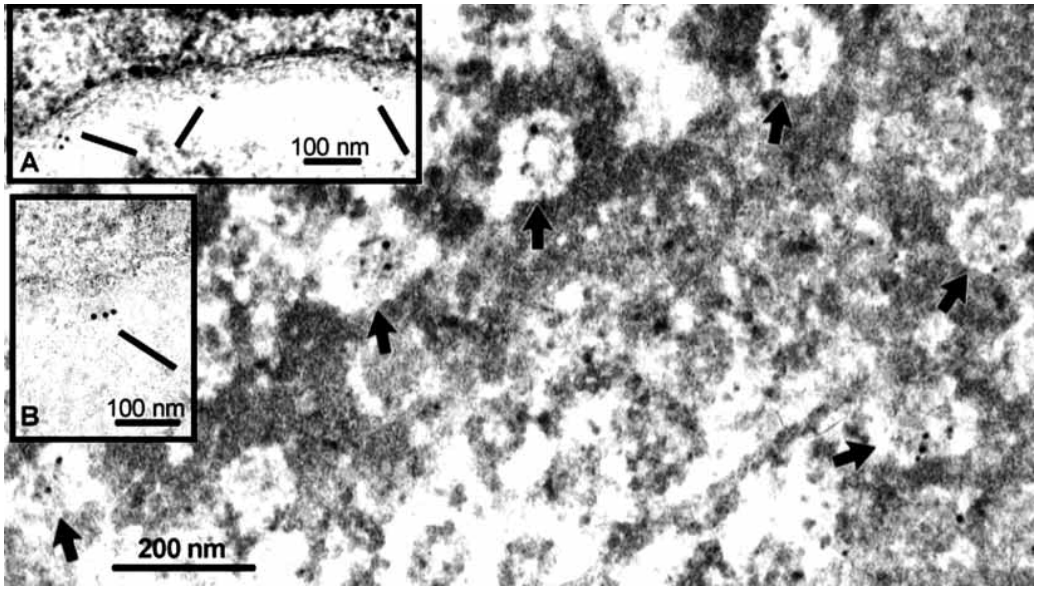

Fig. 6. Immuno-EM localizes HsMAD1 to the nucleoplasmic side of the NPC. HeLa cells were fixed, stained with HsMAD1 antibodies followed by gold-secondary antibodies, and silver enhanced before embedding. NPCs are seen in a surface view of the nuclear envelope, with HsMAD1 labeling indicated by arrows. Insets A and B show cross sections of NPCs with HsMAD1 labeling on filamentous structures on the nucleoplasmic face of the pores.

can be accounted for by the single nucleotide insertion in our HsMAD1 cDNA. The absence of this nucleotide in the TXBP181 cDNA led to a frameshift and altered the predicted amino acid sequence near the carboxy terminus. Thus, an antibody raised against the C-terminal 18 residues would not be expected to recognize endogenous HsMAD1. The antibody generated by Jin et al. recognized a protein of ~150 kDa on western blots (Jin et al., 1998). We believe this was likely some other protein unrelated to HsMAD1. The sequence of TXBP181 predicts a protein of 803 amino acids. Interestingly, it was noted that protein homology to *S. pombe* and *S. cerevisiae* MAD1 extended only over the first 700 or so amino acids. This discrepancy can be resolved because the actual HsMAD1 open reading frame is 718 amino acids. Consistent with this, our affinity purified polyclonal antibodies to HsMAD1 recognize a protein in HeLa cells of approximately 83 kDa, the calculated size.

Our antibodies also yielded a different picture of the cellular distribution of HsMAD1 from that previously published. HsMAD1 is not detected at centromeres during interphase but is localized to nuclear pores based on co-localization with bona fide NPC components and immuno-gold electron microscopic labeling. We clearly demonstrated that HsMAD1 localizes to kinetochores of mitotic chromosomes; it is first detected at kinetochores in prometaphase and is lost upon alignment of chromosomes at the metaphase plate. Differences can be detected within a single prometaphase cell, with HsMAD1 present at kinetochores of unaligned chromosomes and absent from those already at the metaphase plate. Aside from appearing at kinetochores, packets of HsMAD1 can be observed traversing spindle microtubules between chromosomes and centrosomes (Fig. 2). This behavior has also been reported for MAD2. Fluorescently tagged MAD2 can be seen traveling along microtubules from aligned metaphase chromosomes toward the centrosomes in living cells (Howell et al., 2000). We have not established the directionality of HsMAD1 traffic, but HsMAD1 and HsMAD2 seem to have nearly identical localizations throughout mitosis. The dynamic

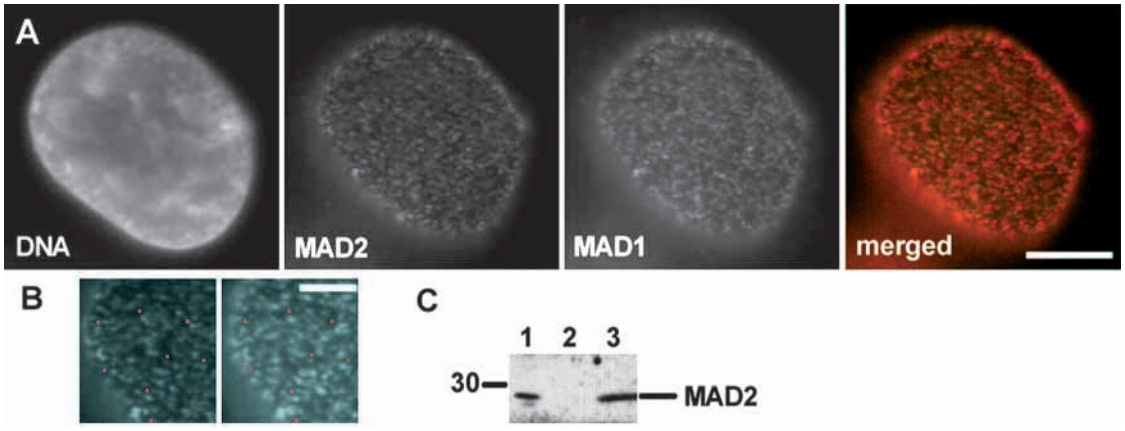

Fig. 7. HsMAD2 co-localizes to nuclear pores with HsMAD1. (A) HeLa cells were double labeled with antibodies to HsMAD2 and HsMAD1. Rabbit anti-HsMAD2 was stained with Cy2 anti-rabbit and rat HsMAD1 antibodies were stained with Cy3-conjugated anti-rat secondary antibodies. DNA was stained with DAPI. Bar, 5 μm. (B) An area of the cell shown in (A) was enlarged to show HsMAD2 (left) and HsMAD1 (right) labeling in more detail, with purple dots shown to aid in registration. Bar, 2.5 μm. (C) Western blots of whole nuclei (lane 1), nuclease and salt extracted supernatant (lane 2), and highly enriched nuclear envelopes (lane 3) from HL60 cells were probed for MAD2.

behavior of these proteins may be evidence for a mitotic checkpoint telegraph system, with spindle microtubules as the wires and the kinetochores and centrosomes as correspondents at each end, that helps transmit signals throughout the mitotic apparatus. These discrepancies between our immunofluorescence results and those reported by Jin et al. (Jin et al., 1998) can be explained by the different specificities of our anti-HsMAD1 antibodies and their anti-TXBP181 antibodies.

We have confirmed, through immunoprecipitation experiments, previous results from human (Jin et al., 1998), yeast (Chen et al., 1999), and *Xenopus* (Chen et al., 1998) that MAD1 associates with MAD2. HsMAD1 antibodies consistently immunoprecipitate MAD2 protein. MAD2 is also known to bind to p55CDC, and this association allows MAD2 to exert its inhibitory effect on the APC/C (Li et al., 1997; Wassmann and Benezra, 1998). Interestingly, we were unable to detect HsMAD1 in p55CDC immunocomplexes that also contained HsMAD2. While this finding does not rule out an association between HsMAD1 and p55CDC, it suggests that any interaction is likely to be fleeting. Interestingly, this appears not to be the case in yeast, where Mad1p, Mad2p, and Cdc20p (p55CDC) are all found in association with each other (Hwang et al., 1998). Jin et al. also reported that, since TXBP181 was able to interact with itself in a yeast two-hybrid screen, 'MAD1 functions as a homodimer' (Jin et al., 1998). We found that transfected GST-HsMAD1 did not appear to form stable dimers with endogenous HsMAD1 (Fig. 3B), which would seem to argue against HsMAD1 dimerization. It is possible, however, that, even though the GST-HsMAD1 fusion protein is able to bind HsMAD2, the GST moiety prevents dimerization of the fusion protein with native HsMAD1.

Mad1p is known to be a phosphoprotein in yeast (Hardwick and Murray, 1995; Hardwick et al., 1996), and can be phosphorylated in mitosis by another essential checkpoint protein, Mps1p kinase (Hardwick et al., 1996). On longer exposures of western blots with our anti-HsMAD1 antibodies we can see an additional band that is of lower molecular mass than the primary HsMAD1 band (not shown). There is no difference in the relative abundance of the bands between interphase and mitosis, so the modification does not appear to be cell cycle-dependent. Further, treatment of samples with lambda phosphatase failed to collapse the two bands into one (not shown), so it is unclear that the difference is due to phosphorylation. These data are consistent with Xmad1, which also does not appear to be phosphorylated in mitosis (Chen et al., 1998).

Perhaps our most interesting and unexpected finding is that both HsMAD1 and HsMAD2 are found at nuclear pore complexes throughout interphase. Although both proteins have been previously described as being at the nuclear envelope (Chen et al., 1996; Chen et al., 1998), we provide the first evidence for the presence of mitotic checkpoint proteins at the nuclear pore complex. The significance of this finding is unclear, but it suggests either that mitotic checkpoint proteins may play distinct roles in other parts of the cell cycle or that the nuclear pore complex plays a role in the operation of the mitotic checkpoint.

We localized HsMAD1 to the nucleoplasmic face of the pore complex. Immunoelectron microscopy revealed that HsMAD1 appears to extend toward the interior of the nucleus from the nuclear envelope. We believe this is consistent with a localization of HsMAD1 within the nucleoplasmic filaments that extend from the NPC to form the basket-like structure. The association of HsMAD1 with the NPC is not likely to be a transient, low affinity one, since it survives the harsh extraction procedures used in isolating nuclear envelopes. HsMAD1 is a prominent component of the purified nuclear envelope fraction (Fig. 4D). One group recently made a tour de force effort to identify every protein of the yeast nuclear pore complex (Rout et al., 2000). Based on redundancies built into their methods, the authors felt confident they had successfully identified all permanent NPC components. Interestingly, Mad1p and Mad2p were not among them. This suggests that yeast Mad1p and Mad2p may not share the NPC localization of their human homologues.

In addition, we found that overexpression of HsMAD1 can drive formation of annulate lamellae, structures thought to represent storage compartments for NPC proteins. This suggests that HsMAD1 can recruit other NPC proteins to build

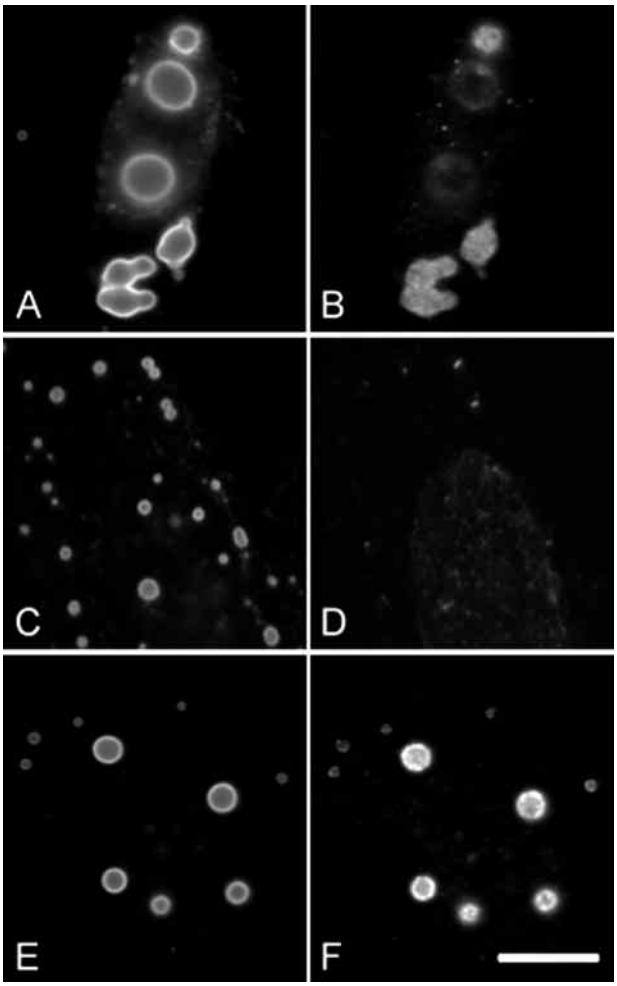

Fig. 8. Overexpression of HsMAD1 causes formation of annulate lamellae containing other NPC proteins. HeLa cells were transfected with GST-HsMAD1 and harvested 24-36 hours later. Cells were labeled with anti-GST (A,C,E) and anti-Nup93 (B), mAb414 (D), and anti-HsMAD2 (F). Bar, 5 μm.

annulate lamellae as well as a possible role for HsMAD1 in the formation of NPCs.

Human MAD1 was first isolated as a binding partner of the HTLV-1 Tax protein, which activates viral and cellular gene expression (Jin et al., 1998). Tax-transformed cells are karyotypically abnormal and often have multiple small nuclei (Majone et al., 1993; Semmes et al., 1996). These characteristics can result from a dysfunctional mitotic checkpoint, so it was proposed that Tax-induced transformation led to aneuploidy by binding to HsMAD1 during mitosis and thereby disrupting its critical mitotic checkpoint function (Jin et al., 1998). The finding that HsMAD1 is an NPC component suggests an additional possibility.

Although the distribution of Tax in cells is not identical to that of HsMAD1, it is concentrated in the nucleus. Tax is present in the interior of the nucleus in speckles that correspond to areas of high transcriptional activity (Semmes and Jeang, 1996). Tax is known to shuttle between the nucleus and the cytoplasm (Burton et al., 2000) and, among its many other abilities, can facilitate the transport of viral DNA into the nucleus (Szabo et al., 1999). These findings suggest that Tax/HsMAD1 interactions may occur at the NPC during interphase in addition to a possible mitotic association. Even though HsMAD1 is truncated relative to TXBP181, the reported Tax binding domain between amino acids 324-498 (Jin et al., 1998) is still present. Although the function of HsMAD1 at NPCs is unknown, Tax binding to HsMAD1 might facilitate its transit through nuclear pores. To our knowledge, no one has examined Tax localization in mitotic cells. Further studies will be required to determine whether the function and localization of HsMAD1, HsMAD2, and other checkpoint proteins are disrupted in Tax-expressing cells.

Two recent reports have identified HsMAD2 as a binding partner of proteins that were not thought to have any mitosis-specific roles. Two-hybrid screens using estrogen receptor beta (Poelzl et al., 2000) and FAT10, a ubiquitin-like molecule (Liu et al., 1999), as bait revealed interactions with HsMAD2. Both groups pointed to association with the mitotic checkpoint protein HsMAD2 to suggest possible alternate roles for ER-beta and FAT10 in cell cycle control. Given that HsMAD2 itself may have non-mitotic functions, however, caution must be exercised in the interpretation of such results.

While our finding that HsMAD1 and HsMAD2 are nuclear pore complex components is a first for checkpoint proteins, it is only the most recent in a series of reports establishing a connection between proteins of the chromosome and spindle apparatus and the nuclear envelope. The budding yeast protein Mps2p, essential for spindle pole body (SPB) duplication, is located at SPBs as well as throughout the nuclear envelope (Munoz-Centeno et al., 1999). The human tankyrase protein, normally associated with telomeres of chromosomes in metaphase, was also found to localize to the pericentriolar area in mitosis and the NPC in interphase (Smith and de Lange, 1999). Using autoimmune sera, Theodoropoulos et al. identified a NPC protein that is also distributed throughout the spindle apparatus in mitosis (Theodoropoulos et al., 1999). The location of a protein within a cell obviously plays an important role in the function of that protein. The multiple localizations of all these proteins suggest they may serve different functions in mitosis and interphase.

Another possibility is that the NPC localization of HsMAD1 and HsMAD2 is in some way related to their mitotic functions. It has long been known that centromeric regions are neither static nor are they randomly distributed throughout interphase nuclei. In fact, interphase centromeres are frequently found associated with the nuclear envelope (Haaf and Schmid, 1989; Ochs and Press, 1992; Li et al., 1997; Moroi et al., 1981; our unpublished observations). One tantalizing possibility is that these associations affect the structure and composition of the centromere/kinetochore complex. For example, HsMAD1 at NPCs may serve as a docking partner for interphase centromeres at the nuclear envelope. During nuclear envelope breakdown at the end of prophase, HsMAD1 and HsMAD2 may lose their associations with the disassembling NPCs and be directly transferred to kinetochores to serve their mitotic checkpoint functions. Alternatively, HsMAD1 might be involved in regulating the nuclear transport of proteins required for entry into mitosis, but this idea would be more compelling if HsMAD1 were present at NPCs only just prior to mitosis. The true role of HsMAD1, as well as HsMAD2, at NPCs must await further experimentation.

We thank Dr E. D. Salmon for providing MAD2 antibodies, Dr F. Melchior for donating a blot of rat nuclear envelope proteins, and Dr J. vanDeursen for providing Nup93 antibodies and critical reading of the manuscript. We are grateful to Dr M. Jarnik and T. Gales for assistance with electron microscopy. M.S.C. gratefully acknowledges the support of a grant from the Cancer Research Fund of the Damon Runyon-Walter Winchell Foundation. This work was also supported by the NIH, ACS, March of Dimes Foundation to T.J.Y. and Core Grant CA 06927 and an appropriation from the Commonwealth of Pennsylvania.

REFERENCES

Alexandru, G., Zachariae, W., Schleiffer, A. and Nasmyth, K. (1999). Sister chromatid separation and chromosome re-duplication are regulated by different mechanisms in response to spindle damage. *EMBO J.* **18**, 2707-2721.

Bodoor, K., Shaikh, S., Enarson, P., Chowdhury, S., Salina, D., Raharjo, W. H. and Burke, B. (1999). Function and assembly of nuclear pore complex proteins. *Biochem. Cell. Biol.* **77**, 321-329.

Burton, M., Upadhyaya, C. D., Maier, B., Hope, T. S. and Semmes, O. J. (2000). Human T-cell leukemia virus type 1 tax shuttles between functionally discrete subcellular targets. *J. Virol.* **74**, 2351-2364.

Chen, R. H., Waters, J. C., Salmon, E. D. and Murray, A. W. (1996). Association of spindle assembly checkpoint component XMAD2 with unattached kinetochores. *Science* **274**, 242-246.

Chen, R. H., Shevchenko, A., Mann, M. and Murray, A. W. (1998). Spindle checkpoint protein Xmad1 recruits Xmad2 to unattached kinetochores. *J. Cell Biol.* **143**, 283-295.

Chen, R. H., Brady, D. M., Smith, D., Murray, A. W. and Hardwick, K. G. (1999). The spindle checkpoint of budding yeast depends on a tight complex between the Mad1 and Mad2 proteins. *Mol. Biol. Cell.* **10**, 2607-2618.

Davis, L. I. and Blobel, G. (1986). Identification and characterization of a nuclear pore complex protein. *Cell* **45**, 699-709.

Fang, G., Yu, H. and Kirschner, M. W. (1999). Control of mitotic transitions by the anaphase-promoting complex. *Philos. Trans. R. Soc. Lond. B. Biol. Sci.* **354**, 1583-1590.

Fesquet, D., Fitzpatrick, P. J., Johnson, A. L., Kramer, K. M., Toyn, J. H. and Johnston, L. H. (1999). A Bub2p-dependent spindle checkpoint pathway regulates the Dbf2p kinase in budding yeast. *EMBO J.* **18**, 2424-2434.

Fraschini, R., Formenti, E., Lucchini, G. and Piatti, S. (1999). Budding yeast Bub2 is localized at spindle pole bodies and activates the mitotic checkpoint via a different pathway from Mad2. *J. Cell Biol.* **145**, 979-991.

Haaf, T. and Schmid, M. (1989). Centromeric association and non-random

distribution of centromeres in human tumour cells. *Hum. Genet.* **81**, 137-143.

Hardwick, K. G. and Murray, A. W. (1995). Mad1p, a phosphoprotein component of the spindle assembly checkpoint in budding yeast. *J. Cell Biol.* **131**, 709-720.

Hardwick, K. G., Weiss, E., Luca, F. C., Winey, M. and Murray, A. W. (1996). Activation of the budding yeast spindle assembly checkpoint without mitotic spindle disruption. *Science* **273**, 953-956.

Hershko, A. (1999). Mechanisms and regulation of the degradation of cyclin B. *Philos. Trans. R. Soc. Lond. B. Biol. Sci.* **354**, 1571-1575.

Howell, B. J., Hoffman, D. B., Fang, G., Murray, A. W., Salmon, E. D. (2000). Visualization of Mad2 dynamics at kinetochores, along spindle fibers, and at spindle poles in living cells. *J. Cell Biol.* **150**, 1233-1250.

Hoyt, M. A., Totis, L. and Roberts, B. T. (1991). S. cerevisiae genes required for cell cycle arrest in response to loss of microtubule function. *Cell* **66**, 507-517.

Hwang, L. H., Lau, L. F., Smith, D. L., Mistrot, C. A., Hardwick, K. G., Hwang, E. S., Amon, A. and Murray, A. W. (1998). Budding yeast Cdc20: a target of the spindle checkpoint. *Science* **279**, 1041-1044.

Imreh, G. and Hallberg, E. (2000). An integral membrane protein from the nuclear pore complex is also present in the annulate lamellae: implications for annulate lamellae formation. *Exp. Cell Res.* **259**, 180-190.

Jin, D. Y., Spencer, F. and Jeang, K. T. (1998). Human T cell leukemia virus type 1 oncoprotein Tax targets the human mitotic checkpoint protein MAD1. *Cell* **93**, 81-91.

Kallio, M., Weinstein, J., Daum, J. R., Burke, D. J. and Gorbsky, G. J. (1998). Mammalian p55CDC mediates association of the spindle checkpoint protein Mad2 with the cyclosome/anaphase-promoting complex, and is involved in regulating anaphase onset and late mitotic events. *J. Cell Biol.* **141**, 1393-1406.

Kaufmann, S. H., Gibson, W. and Shaper, J. H. (1983). Characterization of the major polypeptides of the rat liver nuclear envelope. *J. Biol. Chem.* **258**, 2710-2719.

Kessel, R. G. (1992). Annulate lamellae: a last frontier in cellular organelles. *Int. Rev. Cytol.* **133**, 43-120.

Li, R. and Murray, A. W. (1991). Feedback control of mitosis in budding yeast. *Cell* **66**, 519-531.

Li, X. and Nicklas, R. B. (1995). Mitotic forces control a cell-cycle checkpoint. *Nature* **373**, 630-632.

Li, Y. and Benezra, R. (1996). Identification of a human mitotic checkpoint gene: hsMAD2. *Science* **274**, 246-248.

Li, Y., Gorbea, C., Mahaffey, D., Rechsteiner, M. and Benezra, R. (1997). MAD2 associates with the cyclosome/anaphase-promoting complex and inhibits its activity. *Proc. Nat. Acad. Sci. USA* **94**, 12431-12436.

Liu, Y. C., Pan, J., Zhang, C., Fan, W., Collinge, M., Bender, J. R. and Weissman, S. M. (1999). A MHC-encoded ubiquitin-like protein (FAT10) binds noncovalently to the spindle assembly checkpoint protein MAD2. *Proc. Nat. Acad. Sci. USA* **96**, 4313-4318.

Mahajan, R., Gerace, L. and Melchior, F. (1998). Molecular characterization of the SUMO-1 modification of RanGAP1 and its role in nuclear envelope association. *J. Cell Biol.* **140**, 259-270.

Majone, F., Semmes, O. J. and Jeang, K. T. (1993). Induction of micronuclei by HTLV-I Tax: a cellular assay for function. *Virology* **193**, 456-459.

Moroi, Y., Hartman, A. L., Nakane, P. K. and Tan, E. M. (1981). Distribution of kinetochore (centromere) antigen in mammalian cell nuclei. *J. Cell Biol.* **90**, 254-259.

Munoz-Centeno, M. C., McBratney, S., Monterrosa, A., Byers, B., Mann, C. and Winey, M. (1999). Saccharomyces cerevisiae MPS2 encodes a membrane protein localized at the spindle pole body and the nuclear envelope. *Mol. Biol. Cell.* **10**, 2393-2406.

Ochs, R. L. and Press, R. I. (1992). Centromere autoantigens are associated with the nucleolus. *Exp. Cell Res.* **200**, 339-350.

Pante, N., Bastos, R., McMorrow, I., Burke, B. and Aebi, U. (1994). Interactions and three-dimensional localization of a group of nuclear pore complex proteins. *J. Cell Biol.* **126**, 603-617.

Poelzl, G., Kasai, Y., Mochizuki, N., Shaul, P. W., Brown, M. and Mendelsohn, M. E. (2000). Specific association of estrogen receptor beta with the cell cycle spindle assembly checkpoint protein, MAD2. *Proc. Nat. Acad. Sci. USA* **97**, 2836-2839.

Rieder, C. L., Cole, R. W., Khodjakov, A. and Sluder, G. (1995). The checkpoint delaying anaphase in response to chromosome monoorientation is mediated by an inhibitory signal produced by unattached kinetochores. *J. Cell Biol.* **130**, 941-948.

Rout, M. P., Aitchison, J. D., Suprapto, A., Hjertaas, K., Zhao, Y. and Chait, B. T. (2000). The yeast nuclear pore complex: composition, architecture, and transport mechanism. *J. Cell Biol.* **148**, 635-651.

Semmes, O. J. and Jeang, K. T. (1996). Localization of human T-cell leukemia virus type 1 tax to subnuclear compartments that overlap with interchromatin speckles. *J. Virol.* **70**, 6347-6357.

Semmes, O. J., Majone, F., Cantemir, C., Turchetto, L., Hjelle, B. and Jeang, K. T. (1996). HTLV-I and HTLV-II Tax: differences in induction of micronuclei in cells and transcriptional activation of viral LTRs. *Virology* **217**, 373-379.

Smith, S. and de Lange, T. (1999). Cell cycle dependent localization of the telomeric PARP, tankyrase, to nuclear pore complexes and centrosomes. *J. Cell Sci.* **112**, 3649-3656.

Szabo, J., Beck, Z., Csoman, E., Liu, X., Andriko, I., Kiss, J., Basci, A., Ebbesen, P. and Toth, F. D. (1999). Differential patterns of interaction between HIV type 1 and HTLV type I in monocyte-derived macrophages cultured in vitro: implications for in vivo coinfection with HIV type 1 and HTLV type I. *AIDS Res. Hum. Retroviruses* **15**, 1653-1666.

Taylor, S. S. (1999). Chromosome segregation: dual control ensures fidelity. *Curr. Biol.* **9**, 562-564.

Theodoropoulos, P. A., Polioudaki, H., Koulentaki, M., Kouroumalis, E. and Georgatos, S. D. (1999). PBC68: a nuclear pore complex protein that associates reversibly with the mitotic spindle. *J. Cell Sci.* **112**, 3049-3059.

Wassmann, K. and Benezra, R. (1998). Mad2 transiently associates with an APC/p55CDC complex during mitosis. *Proc. Nat. Acad. Sci. USA* **95**, 11193-11198.

Weiss, E. and Winey, M. (1996). The Saccharomyces cerevisiae spindle pole body duplication gene MPS1 is part of a mitotic checkpoint. *J. Cell Biol.* **132**, 111-123.

Winey, M., Goetsch, L., Baum, P. and Byers, B. (1991). MPS1 and MPS2: novel yeast genes defining distinct steps of spindle pole body duplication. *J. Cell Biol.* **114**, 745-754.